Journal of Photochemistry and Photobiology A: Chemistry 253 (2013) 52–61

Contents lists available at SciVerse ScienceDirect

Journal of Photochemistry and Photobiology A: Chemistry

journal homepage: www.elsevier.com/locate/jphotochem

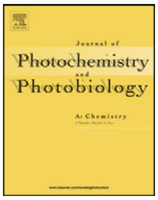

Photoprocesses in styryl dyes and their pseudorotaxane complexes with cucurbit[7]uril

Levon S. Atabekyan, Artem I. Vedernikov, Vitaly G. Avakyan, Natalia A. Lobova,
Sergey P. Gromov*, Alexander K. Chibisov*

Photochemistry Center, Russian Academy of Sciences, 7A-1 Novatorov str., 119421 Moscow, Russia

ARTICLE INFO

Article history:
Received 14 August 2012
Received in revised form
10 December 2012
Accepted 15 December 2012
Available online 6 January 2013

Keywords:
Styryl dyes
Cucurbit[7]uril
Inclusion complexes
Stability constants
Triplet states
Fluorescence

ABSTRACT

The formation of inclusion complexes between styryl dyes containing a dimethylamino group or azacrown-ether residue and cucurbit[7]uril (CB[7]) in aqueous solution was studied by ^{1}H NMR spectroscopy and quantum chemistry. The complexes are characterized by 1:1 composition and the pseudorotaxane structure, which was confirmed by quantum chemical calculations. The free dyes and dye@CB[7] complexes exhibit both prompt fluorescence and an ability to intersystem crossing. The triplet–triplet absorption spectra and the triplet lifetime of the free dyes and dye@CB[7] were measured by ns-laser photolysis.

1. Introduction

Styryl dyes of the general formula R—Het$^+$—CH═CH—Ar X$^-$ can undergo *E*–*Z* isomerization, electrocyclization and [2 + 2] cycloaddition photoreactions owing to the presence of ethylene bonds in the dye molecules [1–5]. The photochemical properties of styryl dyes were studied in a number of publications [6–11]; however, several aspects of the mechanism of the primary photoreactions remained unclear. Data on the short-lived intermediates are missing either. Lately, the complexation of dyes of various classes with macroheterocyclic cavitands, cucurbit[*n*]urils (CB[*n*]), has been vigorously studied [12–14]. It was found [11,15–17] that the formation of inclusion complexes of styryl dyes with CB[6] and CB[7] affects the spectral and luminescence properties of the dyes, in particular, results in substantial enhancement of fluorescence. The latter was also observed in the formation of inclusion complexes of styryl dyes with other cavitand molecules, for example, cyclodextrins [18–27]. In particular, we studied the influence of 2-hydroxypropyl-β-cyclodextrin (HP-β-CD) on spectral and luminescent properties of neutral crown-containing 2-styrylbenzothiazole (CSB) in water [23]. It was shown that the fluorescence intensity of CSB is enhanced with increasing of HP-β-CD concentration that clearly demonstrates the formation of 1:1 inclusion complex CSB@HP-β-CD. The quantum yield of CSB fluorescence is five-times increased in the presence of HP-β-CD. The stoichiometry of inclusion complex was found to be 1:1 for concentration of HP-β-CD varied up to 0.004 M. The value of stability constant for this complex is changed from log*K* = 3.64 to log*K* = 3.47 in the 10–40 °C temperature range [23].

Recently we found that 4-pyridine styryl dyes with a dimethylamino group ((*E*)-**1**) or an aza-18-crown-6-ether residue ((*E*)-**2**) demonstrate an ability to intersystem crossing. Along with radiationless decay of the triplet state the phosphorescence and delayed fluorescence also make a contribution in the overall triplet decay. It was pointed out that the vibration relaxation of the Franck–Condon excited state resulted in the planar intramolecular charge transfer (PICT). The following pathways of PICT deactivation are the intersystem crossing, fluorescence and transition to the twisted intramolecular charge transfer (TICT) [28]. To our best knowledge no data are available in the literature on the influence of CB[*n*] on the efficiency of intersystem crossing of styryl dye molecules. Therefore, it appears important to study the effect of CB[*n*] on the primary photoprocesses in styryl dye complexes Scheme 1.

In this paper, we present the results on a study of the photophysical properties of dyes (*E*)-**1** and (*E*)-**2** and their complexes

---

* Corresponding authors. Tel.: +7 495 9361204; fax: +7 495 9361255.
E-mail addresses: alexander.chibisov@gmail.com, chibisov@photonics.ru (A.K. Chibisov).

1010-6030/$ – see front matter © 2013 Elsevier B.V. All rights reserved.
http://dx.doi.org/10.1016/j.jphotochem.2012.12.023

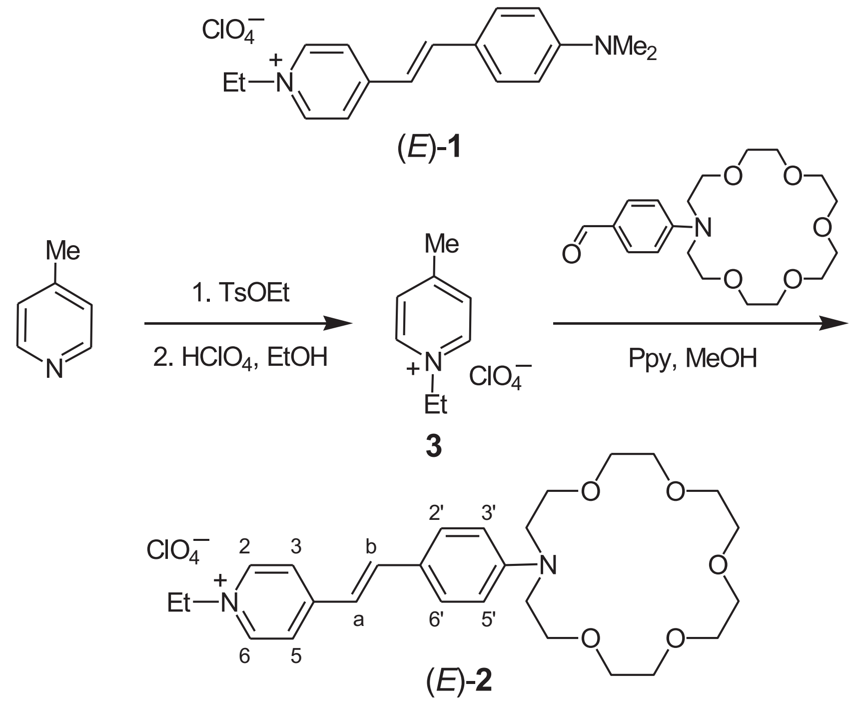

Scheme 1.

with CB[7] in aqueous solutions. The principal result of this work is that complexes are characterized by 1:1 composition and the pseudorotaxane structure which is confirmed by quantum chemical calculations. The complexes dye@CB[7] show both prompt fluorescence and an ability to intersystem crossing and the triplet lifetime of dye@CB[7] is close to that of free dye.

2. Experimental

2.1. Materials

The synthesis of dye (*E*)-**1** was described earlier [4]. Ethyl *p*-toluenesulfonate, 70% $HClO_4$ (aq), *N*-(4-formylphenyl)aza-18-crown-6 ether, CB[7]·$13H_2O$, and fluorescein were used as received (Aldrich). Distilled water (HPLC grade, Aldrich), acetonitrile (extra high purity, Cryochrom), and Li_2CO_3 (Merck) were used to prepare solutions.

2.1.1. 1-Ethyl-4-methylpyridinium perchlorate (3)

A mixture of 4-picoline (1.0 mL, 10.3 mmol) and ethyl *p*-toluenesulfonate (3.07 g, 15.4 mmol) was heated at 120 °C (oil bath) for 1 h. The resulting mass was dissolved in hot abs. EtOH (5 mL), and 70% $HClO_4$ (aq) (1.77 mL, 20.5 mmol) was added to the ethanolic solution. The mixture was cooled to −10 °C and a yellowish glassy precipitate was separated by decantation, washed with hot benzene (3 × 20 mL), and re-crystallized from abs. EtOH. The yield of **3** was 0.68 g (30%), m.p. 56–58 °C.

^1H NMR (500 MHz, DMSO-d_6) 30 °C, δ: 1.51 (t, 3H, *J* = 7.5 Hz, *Me*CH_2); 2.60 (s, 3H, Me); 4.55 (q, 2H, *J* = 7.5 Hz, CH_2N); 7.98 (d, 2H, *J* = 6.6 Hz, 3-H, 5-H); 8.91 (d, 2H, *J* = 6.6 Hz, 2-H, 6-H). ^{13}C NMR (125 MHz, DMSO-d_6) 25 °C, δ: 16.09 (*Me*CH_2); 21.21 (Me); 55.46 (CH_2N); 128.27 (3-C, 5-C); 143.36 (2-C, 6-C); 158.61 (4-C). Anal. calcd. for $C_8H_{12}ClNO_4$: C, 43.35; H, 5.46; N, 6.32; found: C, 43.32; H, 5.50; N, 6.25%.

2.1.2. 1-Ethyl-4-{(E)-2-[4-(1,4,7,10,13-pentaoxa-16-azacyclooctadecan-16-yl)phenyl]vinyl}pyridinium perchlorate ((E)-2)

A solution of a mixture of compound **3** (181 mg, 0.82 mmol), *N*-(4-formylphenyl)aza-18-crown-6 ether (330 mg, 0.90 mmol) and piperidine (40 μL) in MeOH (10 mL) was heated at 65 °C (oil bath) for 20 h and then cooled to −10 °C. A dark-red glassy solid was separated by decantation, washed with hot benzene (3 × 20 mL), and dried in vacuo. The yield of (*E*)-**2** was 296 mg (63%), m.p. 64–66 °C.

^1H NMR (500 MHz, DMSO-d_6) 30 °C, δ: 1.50 (t, 3H, *J* = 7.3 Hz, Me); 3.53 (s, 8H, 4CH_2O); 3.54 (m, 4H, 2CH_2O); 3.55 (m, 4H, 2CH_2O); 3.63 (m, 8H, $(CH_2)_2N$, 2CH_2O); 4.44 (q, 2H, *J* = 7.3 Hz, CH_2Me); 6.79 (d, 2H, *J* = 8.9 Hz, 3′-H, 5′-H); 7.14 (d, 1H, *J* = 16.2 Hz, CH = *CH*Py); 7.57 (d, 2H, *J* = 8.9 Hz, 2′-H, 6′-H); 7.89 (d, 1H, *J* = 16.2 Hz, *CH* = CHPy); 8.04 (d, 2H, *J* = 6.9 Hz, 3-H, 5-H); 8.76 (d, 2H, *J* = 6.9 Hz, 2-H, 6-H). ^{13}C NMR (125 MHz, DMSO-d_6) 30 °C, δ: 15.96 (Me); 50.57 ($(CH_2)_2N$); 54.54 (CH_2N); 67.74 ($(OCH_2CH_2)_2N$); 69.82 (2CH_2O); 69.89 (2CH_2O); 69.95 (4CH_2O); 111.57 (3′-C, 5′-C); 116.83 (CH = CHPy); 122.21 (1′-C); 122.28 (3-C, 5-C); 130.25 (2′-C, 6′-C); 141.83 (*C*H = CHPy); 143.07 (2-C, 6-C); 149.83 (4′-C); 153.57 (4-C). Anal. calcd. for $C_{27}H_{39}ClN_2O_9$: C, 56.79; H, 6.88; N, 4.91; found: C, 56.71; H, 6.87; N, 4.88%.

2.2. Methods

Melting points were measured on a Mel-Temp II instrument. Elemental analyses were carried out at the Microanalytical Laboratory of the A.N. Nesmeyanov Institute of Organoelement Compounds (Russian Academy of Sciences, Moscow).

2.2.1. NMR spectroscopy measurements and titration

The ^1H and ^{13}C NMR spectra were recorded on a Bruker DRX500 spectrometer in DMSO-d_6 and a D_2O–MeCN-d_3 mixture (10:1, v/v) at 25–30 °C with the solvent or the HOD signal as the internal standard (δ_H 2.50 or 4.70, respectively; δ_C 39.43 for DMSO-d_6). In ^1H NMR titration, the compositions and stability constants of the complexes of dyes (*E*)-**1**, (*E*)-**2** with CB[7] were determined by analyzing the changes in the positions of the H signals ($\Delta\delta_H$) of the dye depending on the concentration ratio of CB[7] and the dye. The CB[7] concentration was varied in the range from 0 to 1×10^{-3} mol L^{-1}, while the overall concentration of dye did not change remaining equal to $\sim 5 \times 10^{-4}$ mol L^{-1}. The $\Delta\delta_H$ values were measured to an accuracy of 0.001 ppm with correction for MeCN-d$_2$ signal shift. The stability constants of the complexes were calculated using the HYPNMR program [29].

2.2.2. Quantum chemical calculations

The quantum chemical calculations of the structures of CB[7] and dyes **1**, **2** and the structures and the formation enthalpies of complexes dye@CB[7] were carried out by DFT with the exchange-correlation PBE functional [30] in a three-exponent basis set [31] by a reported program [32] and with zero-point energy (ZPE) correction.

2.2.3. Optical spectroscopy measurements and titrations

The spectra of triplet–triplet absorption and the kinetics of triplet decay of dyes (*E*)-**1**, (*E*)-**2** and the complexes with CB[7] were measured on a nanosecond laser photolysis setup [10]. The irradiation was performed with the Nd:YAG laser (Solar, λ = 355 nm, $E \leq 70$ mJ, 15 ns) in quartz cells $1 \times 1 \times 4$ cm^3. The dissolved oxygen was removed by bubbling with nitrogen. The absorption spectra of dyes (*E*)-**1**, (*E*)-**2** and their complexes with CB[7] in the ground state were recorded on an Agilent 8453 as well as a Cary 4000 spectrophotometers. Fluorescence emission and fluorescence excitation spectra were measured on a Varian Eclipse spectrofluorimeter. All the spectra were recorded in deionized water at room temperature. The fluorescence quantum yield was measured by comparison [33] with the standard (fluorescein). The concentrations of (*E*)-**1** and (*E*)-**2** were $(0.4–3) \times 10^{-5}$ mol L^{-1}, and the CB[7] concentration was $(0.4–2) \times 10^{-4}$ mol L^{-1}.

The spectrophotometric and fluorescent titrations were performed in water–MeCN (10:1, v/v) containing 0.01 M Li_2CO_3 at room temperature. The compositions and stability constants of the complexes of dyes (*E*)-**1**, (*E*)-**2** with CB[7] were determined by analyzing the changes in the absorption and fluorescence spectra of the dye depending on the concentration ratio of CB[7] and the dye. In spectrophotometric titration, the CB[7] concentration was varied in the range from 0 to 1.3×10^{-4} mol L^{-1}, while the overall concentration of dye was 2×10^{-5} mol L^{-1}. In fluorescent titration, the CB[7] concentration was changed in the range from 0 to 1.8×10^{-4} mol L^{-1}, and the overall concentration of dye remained equal to 1×10^{-5} mol L^{-1}. The stoichiometry and stability constants of complexes were calculated using HypSpec software (Hyperquad) [34].

3. Results and discussion

3.1. ^{1}H NMR spectroscopy studies

A ^{1}H NMR study of the complexation of dyes (*E*)-**1**, (*E*)-**2** with CB[7] provides data on the structures and thermodynamic stability of supramolecular complexes. To increase the dye solubility to the millimolar range, a D_2O–MeCN-d$_3$ mixture (10:1, v/v) was used [15]. Fig. 1 shows the ^{1}H NMR spectra of free dye (*E*)-**2** and its mixture with excess CB[7]. It can be seen that signals of the (*E*)-**2**/CB[7] mixture differ significantly in the direction and the magnitude of their shifts relative to similar signals of free (*E*)-**2**. Thus the signals of the *N*-ethylpyridinium residue and the ethylene bond shift upfield ($\Delta\delta_H$ of up to −0.89 ppm), while the signals of the benzene ring protons, conversely, shift downfield ($\Delta\delta_H$ of up to 0.25 ppm). This means that the CB[7] molecule shields to the highest extent the protons of the Et—Py$^+$—CH═CH moiety and, thus, the cavitand molecule in the complex is mainly arranged above the positively charged area of the dye molecule. With increasing distance from the center of the Py$^+$—CH═CH moiety, the dye protons become less shielded, and the signals of the benzene ring shift downfield, probably due to the deshielding influence of the carbonyl groups of the host molecule portals. The signals of the most remote protons of the azacrown-ether residue are little sensitive to complexation. This pattern of variation of the magnitude and sign of $\Delta\delta_H$ attests to the pseudorotaxane structure of complex (*E*)-**2**@CB[7] where one end of the guest molecule is located inside the CB[7] cavity, while the other end is outside the cavity. The changes in the ^{1}H NMR spectra of dyes (*E*)-**1** and (*E*)-**2** following the complex formation with CB[7] proved to be similar. Complex (*E*)-**1**@CB[7] has a structure similar to that of complex (*E*)-**2**@CB[7]; however, substantial line broadening is observed in the spectra due to the slower exchange on the ^{1}H NMR time scale as compared with the (*E*)-**2**/CB[7] system.

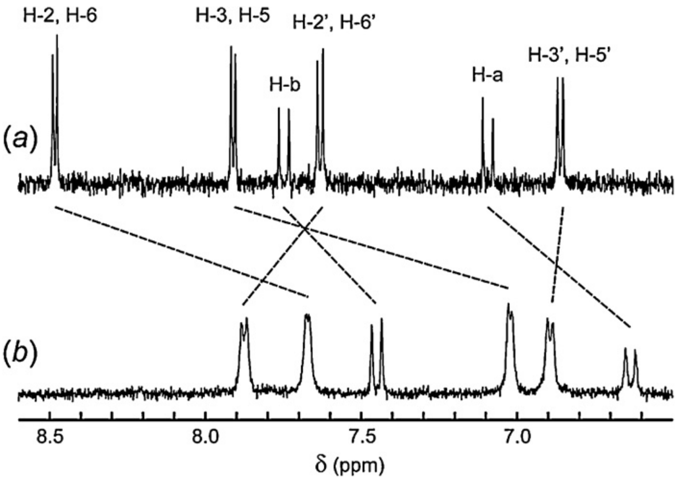

Fig. 1. ^{1}H NMR spectra (aromatic proton region) of (a) free dye (*E*)-**2** and (b) 1:1.5 mixture of (*E*)-**2** and CB[7] ($C_2 = 5 \times 10^{-4}$ mol L^{-1}) in a D_2O–MeCN-d$_3$ mixture (10:1, v/v) at 25 °C.

The stability constants of complexes dye@CB[7] were determined by ^{1}H NMR titration. The dependence of $\Delta\delta_H$ of the dye protons on the change in the cucurbituril and dye concentration ratio was described by a model that took into account a single equilibrium:

$$\text{dye} + \text{CB[7]} \overset{K}{\rightleftarrows} \text{dye@CB[7]}$$

where K is the stability constant of complex dye@CB[7] [L mol^{-1}].

The stability constants of complexes (*E*)-**1**@CB[7] and (*E*)-**2**@CB[7] turned out to be similar: $\log K = 4.3 \pm 0.1$ and 4.4 ± 0.1, respectively. Previously [15,16], by the example of a styryl dye with two methoxy groups in the benzene ring, it was shown that replacement of a D_2O–MeCN-d$_3$ mixture (10:1, v/v) by water increases the stability constant of the dye complex with CB[7] by 1.9 logarithmic units. Probably, the increase in the stability constant of the complex is caused by increase in the polarity of the medium on passing from aqueous acetonitrile to neat water, which promotes the location of the hydrophobic guest molecule in the cavitand cavity. Presumably, the stability of complexes (*E*)-**1**@CB[7] and (*E*)-**2**@CB[7] in water will also be 1–2 orders of magnitude higher that their stability in a water–acetonitrile mixture (10:1, v/v).

3.2. Quantum chemical simulation

The quantum chemical calculations of the structures **1** and **2** in the ground state indicate the possible existence of two dye isomers, namely *E* and *Z* forms. Fig. 2 shows the calculated structures and

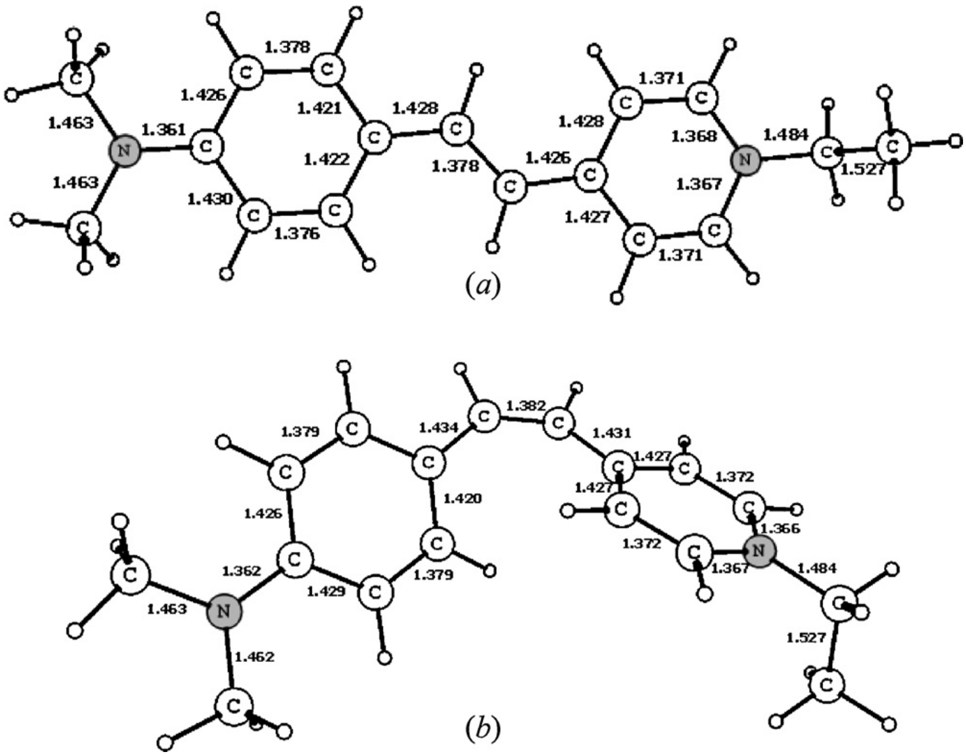

Fig. 2. Structures of (a) *E* and (b) *Z* isomers of dye **1** calculated by DFT/PBE method.

the bond lengths (in Å) for (*E*)-**1** and (*Z*)-**1**. Nearly the same bond lengths were found for the chromophore parts of (*E*)-**2** and (*Z*)-**2**, which are therefore not given here.

The *Z* forms of both dyes are non-planar due to the proximity of the hydrogen atoms of the pyridine and benzene rings of the dyes (see Fig. 2b). The local energy minima characterized by the absence of imaginary frequencies correspond to structures (*Z*)-**1** and (*Z*)-**2** with the dihedral angles $\tau_{CC=CC}$ of 19.1 and 19.6°, respectively. Furthermore, the *E* forms of dyes **1** and **2** are thermodynamically more favorable than the *Z* forms by $\Delta H = 8.3$ and 8.2 kcal mol^{-1}, respectively.

Quantum chemical calculations of the structure and the energy of formation of complexes **1**@CB[7] and **2**@CB[7] were carried out. Each dye and CB[7] molecules were located in three different starting positions. The following dye moieties were placed inside the host cavity: (a) pyridinium residue, (b) aniline residue, (c) central ethylene bond. The starting structures of the complexes were obtained by the semiempirical PM3 method with standard parameters [35]. The calculation showed that the optimal structure of complexes dye@CB[7] corresponded to the structures presented in Fig. 3.

The absence of imaginary frequencies confirmed that the structures found by calculations corresponded to energy minima. It can be seen from Fig. 3 that in both complexes, the vinylpyridinium moiety of the dye is located inside the cavity. This result is in good agreement with ^{1}H NMR data and with the view that cucurbituril hosts form more stable inclusion complexes with positively charged molecules than with related neutral compounds. The energies of insertion of (*E*)-**1** and (*E*)-**2** into the CB[7] cavity, ΔE_0, turned out to be similar (−39.5 and −39.0 kcal mol^{-1}), as was to be expected, because both dyes are inserted in the cavitand with the same moiety. The distances between the C=C bond midpoint and the center of gravity of CB[7], Δl, were 1.99 and 1.96 Å for (*E*)-**1**@CB[7] and (*E*)-**2**@CB[7], respectively. The insertion energies for (*Z*)-**1**@CB[7] and (*Z*)-**2**@CB[7] were −37.7 and −32.1 kcal mol^{-1}, respectively, i.e., they changed little as compared with ΔE_0 for (*E*)-**1**@CB[7] and (*E*)-**2**@CB[7]. The decrease in ΔE_0 by 5.6 kcal mol^{-1} for **2**@CB[7] on going from (*E*)-**2** to (*Z*)-**2** is apparently due to its more pronounced steric repulsion from the cavitand molecule caused by more bulky crown-ether residue. This is consistent with the fact that (*Z*)-**1** is inserted much more deeply than (*Z*)-**2** into the CB[7] cavity. The Δl value for the former was 1.78 Å (~0.2 Å shorter than $\Delta l_{(E)\text{-}\mathbf{1}}$), whereas for the latter Δl was 4.02 Å (more than ~2.0 Å longer than $\Delta l_{(E)\text{-}\mathbf{2}}$).

3.3. Absorption and fluorescence spectra

The measurements of the absorption spectra revealed two peaks at 265 and 450 nm in the spectrum of (*E*)-**1** in water (Fig. 4). The absorption spectrum of (*E*)-**2** nearly coincides with the spectrum of (*E*)-**1**. Dyes **1** and **2** exhibit weak fluorescence at $\lambda_{max} \sim 600$ nm (Fig. 5).

The fluorescence excitation spectrum of **1** ($\lambda_{max} = 480$ nm) differs from the absorption spectrum ($\lambda_{max} = 450$ nm); the same is true for **2**. The difference between the absorption and excitation spectra can be attributed to the presence of two dye isomers one of which does not fluoresce. Indeed, the quantum chemical calculations of structures **1** and **2** indicate the existence of two isomeric forms of the dye, *E* and *Z* forms (see Fig. 2).

The low fluorescence intensity is assumed to be due to the formation of a twisted intramolecular charge transfer (TICT) state upon photoexcitation, similar to that formed for styryl dyes whose structures resemble **1** [17,36–39]. A common feature of the molecules giving rise to the TICT state is the presence of electron-donating and electron-withdrawing groups and a conjugation chain, which facilitates the shift of electron density from the donor to the acceptor upon photoexcitation [39]. The aniline nitrogen atom usually serves as the electron donor whereas nitrile and ester groups or heterocyclic residues as electron acceptors. The structure of **1** fully meets these conditions. The high formation rate

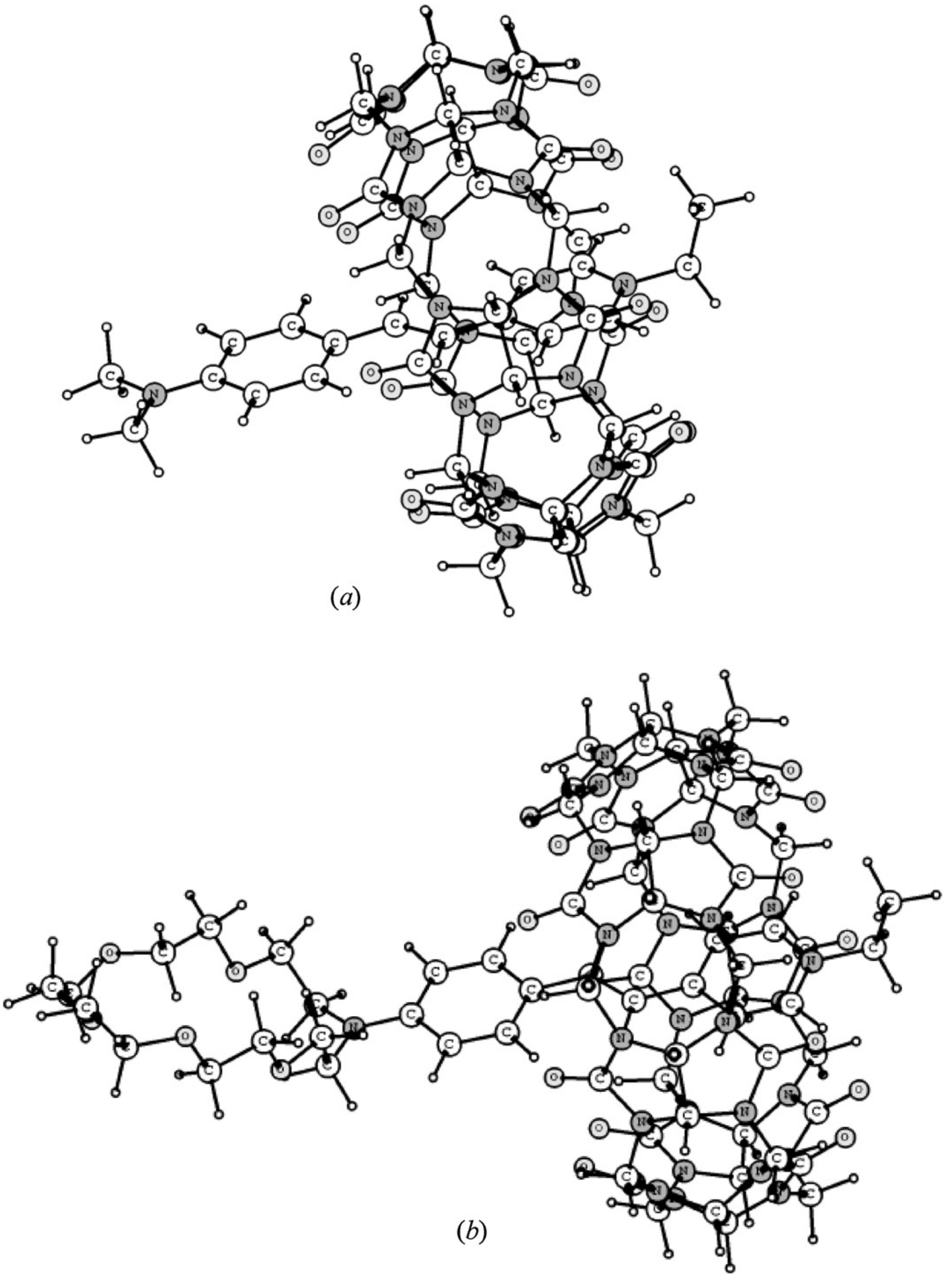

Fig. 3. DFT-calculated structures of complexes (a) (*E*)-**1**@CB[7] ($\Delta E_0 = -39.5$ kcal mol^{-1}) and (b) (*E*)-**2**@CB[7] ($\Delta E_0 = -39.0$ kcal mol^{-1}).

of the TICT state results in a decrease in the photostationary concentration of the singlet excited *E* isomers and, as a consequence, a decrease in the fluorescence. An increase in the fluorescence of **2** can be the reason of lower efficiency of the formation of the TICT state as compared with **1**.

Note the abnormally great Stokes shift of the fluorescence spectrum (130 nm) (Fig. 5) observed for **1** and **2**. This type of shift noted previously [6,17,40,41] for similar compounds may be due to the strong solvatochromic effect. The fluorescence and fluorescence excitation spectra for **1** and **2** resemble each other in pairs, as was to be expected since excitation occurs in the chromophore part of the molecule (Table 1).

The formation of complexes dye@CB[7] induces changes in the absorption spectra with respect to those of free dyes. System (*E*)-**1**/CB[7] typically shows a bathochromic shift of the long-wavelength absorption band and a new band at 330 nm (Fig. 4). The spectral changes in the case of (*E*)-**1**/CB[7] mixture were more pronounced than those of (*E*)-**2**/CB[7]. The absorption with a maximum at 330 nm is due to the complex formed by the protonated form (dye·H)$^+$@CB[7]. This is supported by the absorption spectra of (*E*)-**1** recorded in the presence of $HClO_4$ (see inset in Fig. 4).

The absorption and fluorescence spectra of (*E*)-**2** measured in the presence and in the absence of barium perchlorate are

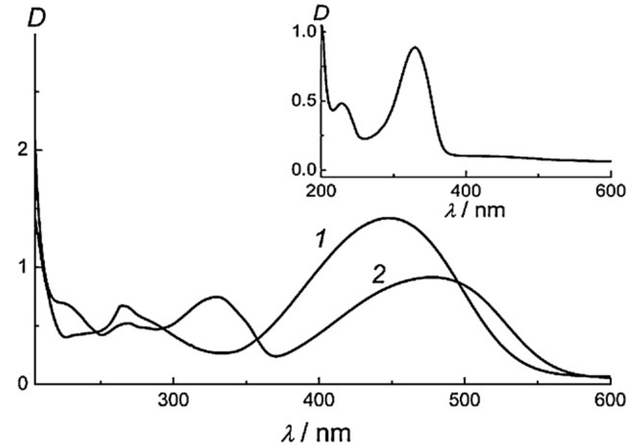

Fig. 4. Absorption spectra of dye (*E*)-**1** ($C_1 = 2 \times 10^{-5}$ mol L^{-1}) in the absence (1) and presence (2) of CB[7] ($C_{CB[7]} = 2 \times 10^{-4}$ mol L^{-1}) in aqueous solution. Inset: the absorption spectrum of dye (*E*)-**1** in the presence of $HClO_4$ (pH = 2).

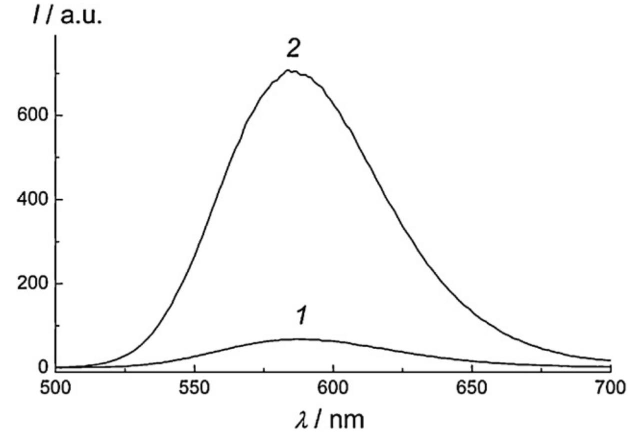

Fig. 6. Fluorescence spectra of dye **2** ($C_2 = 4 \times 10^{-6}$ mol L^{-1}): (1) free dye and (2) in the presence of CB[7] ($C_{CB[7]} = 2 \times 10^{-4}$ mol L^{-1}) in aqueous solution.

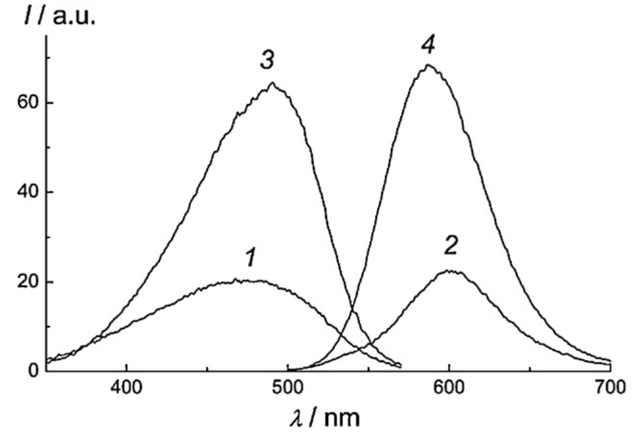

Fig. 5. Fluorescence excitation (1 and 3) and fluorescence emission (2 and 4) spectra of dye **1** (1 and 2) and dye **2** (3 and 4) ($C_{dye} = 4 \times 10^{-6}$ mol L^{-1}) in aqueous solution.

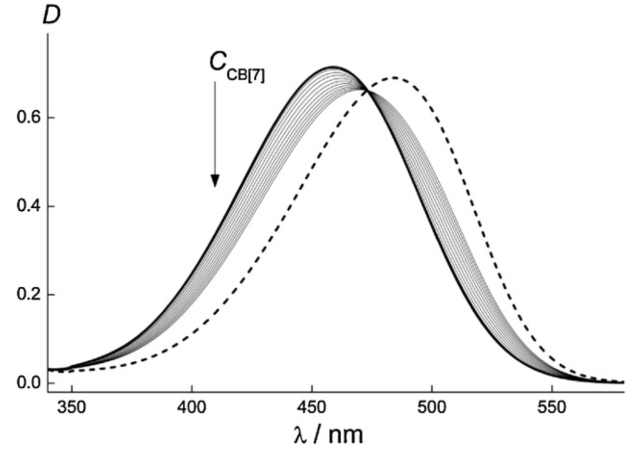

Fig. 7. Absorption spectra of dye (*E*)-**2** ($C = 2 \times 10^{-5}$ mol L^{-1}) in the mixture of water–MeCN (10:1, v/v) with 0.01 M Li_2CO_3 measured for different concentration of CB[7] (0–1.25 × 10^{-4} mol L^{-1}): dotted curve-evaluated spectrum of (*E*)-**2**@CB[7].

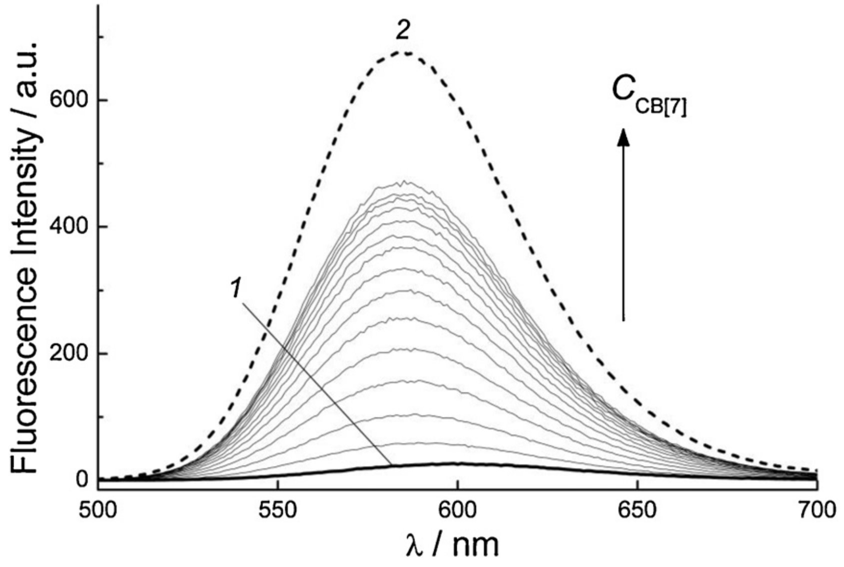

Fig. 8. Fluorescence spectra of dye **2** ($C = 1 \times 10^{-5}$ mol L^{-1}) in the mixture of water–MeCN (10:1, v/v) with 0.01 M Li_2CO_3 measured for different concentration of CB[7] (0–1.80 × 10^{-4} mol L^{-1}); curve 1-fluorescence spectrum of dye **2**, curve 2-evaluated fluorescence spectrum of **2**@CB[7].

identical, which means that no complex (*E*)-**2**@Ba(ClO_4)$_2$ is formed in aqueous solution.

It is noteworthy that in the presence of CB[7], the long-wavelength absorption maximum of (*E*)-**1** and (*E*)-**2** coincides with the maximum of the fluorescence excitation spectrum measured for both dyes in the absence of CB[7] (Fig. 5). Apparently, the formation of the host–guest complex stabilizes the planar *E* isomer of the dye, which is responsible for fluorescence. Fig. 6 shows the fluorescence spectra of **2** and its mixture with CB[7], and Table 1 summarizes the fluorescence and fluorescence excitation maxima and the fluorescence quantum yields measured for **1**, **2**, and their mixtures with CB[7].

Mixtures **1**/CB[7] and **2**/CB[7] show a 8- and 30-fold increase in the fluorescence intensity, respectively, as compared with free dyes (Fig. 6, Table 1), and as also was found for dyes of various types [11,16,42–47]. Previously it has been shown that the inclusion complex of CSB with HP-β-CD demonstrated a five-fold increase of fluorescence, however, the stability constant appeared to be noticeably smaller (log$K$ = 3.5) [23]. One might suppose that the using of CB[7] as a host molecule results in the formation of more strong complex for dyes with the structure close to dyes (*E*)-**1** and (*E*)-**2**.

Thus, the formation of the TICT state, which competes with the radiative deactivation of the excited state of **1** and **2**, is considerably hindered in the presence of CB[7] due to stabilization of the planar conformation of the (*E*)-dye in the host cavity, and this results in considerable increase in the fluorescence quantum yield of the complexes.

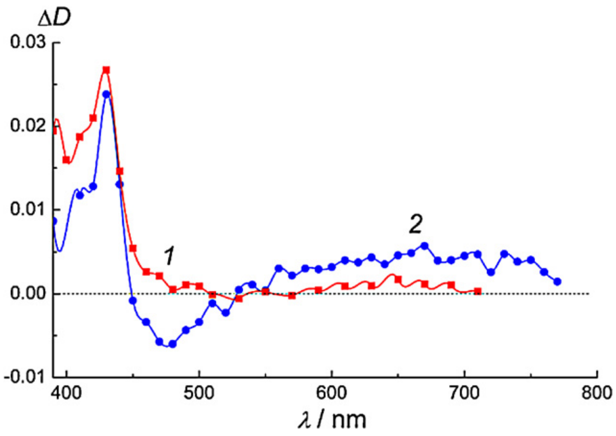

Fig. 10. Transient absorption spectra of dye **1** ($C_1 = 3 \times 10^{-5}$ mol L^{-1}) in aqueous solution at 30 μs after the laser pulse in the presence of $HClO_4$ at (1) pH = 2 and (2) pH = 4.2.

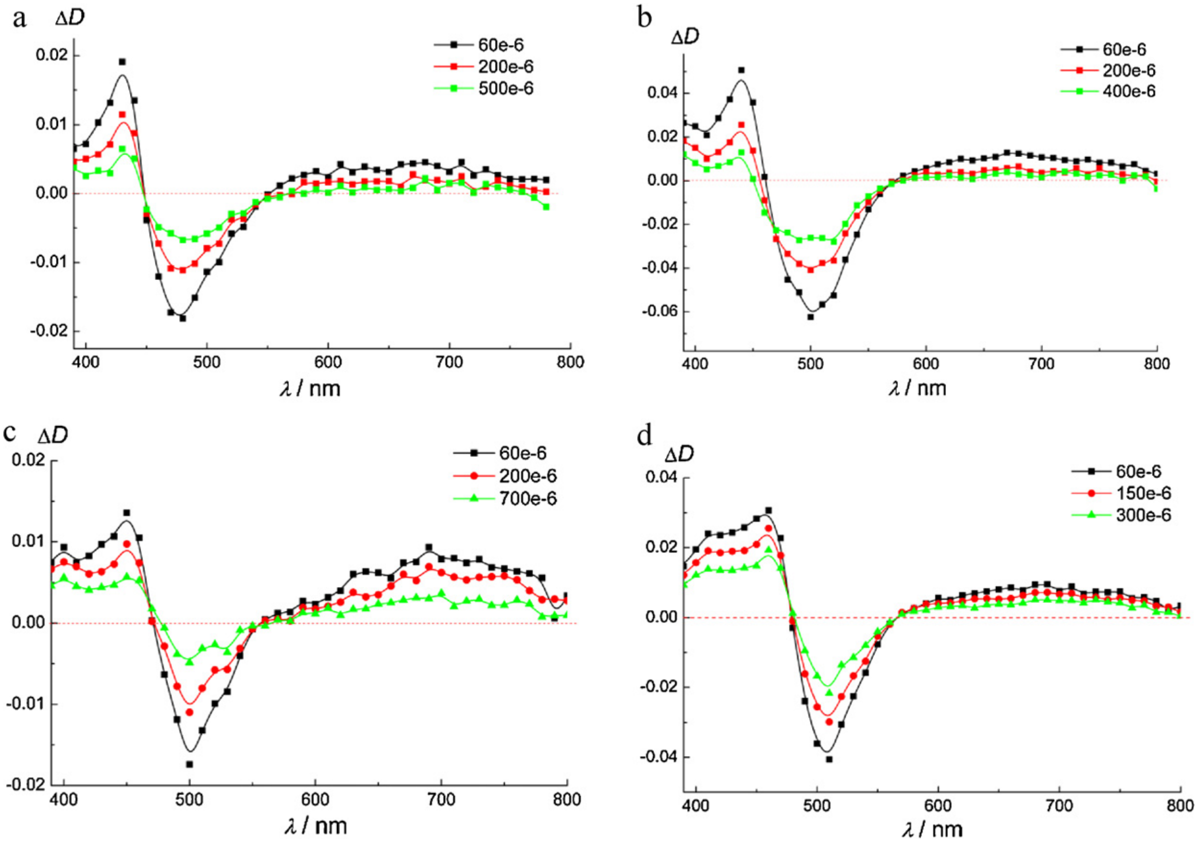

Fig. 9. Transient absorption spectra of (a and b) **1** and (c and d) **2** ($C_{dye} = 2 \times 10^{-5}$ mol L^{-1}) in aqueous solution in the absence (a and c) and presence (b and d) of CB[7] ($C_{CB[7]} = 2 \times 10^{-4}$ mol L^{-1}) at different time (s) after the laser pulse.

3.4. Spectrophotometric and fluorescent titrations

The stability constants of complexes (*E*)-**1**@CB[7] and (*E*)-**2**@CB[7] were also determined by spectrophotometric and fluorescent titrations in a mixture of water–MeCN (10:1, v/v). In the course of titration, the absorbance was decreased at 455 nm and increased at 332 nm with increasing of CB[7] concentration. Evidently the remaining amount of acid in CB[7] promotes the protonation of the dye molecule at aniline nitrogen atom that makes difficult to determine the stability constant. In order to exclude the processes caused by the protonation of dyes **1** and **2** the titrations were performed in the presence of 0.01 M Li_2CO_3. In the course of spectrophotometric titration, a bathochromic shift of the maximum of the long-wavelength absorption band of dye and isosbestic point were observed (see, for example, Fig. 7). With increase of $C_{CB[7]}/C_{dye}$ ratio a strong enhancement of fluorescence was found (Fig. 8) along

Table 1
Spectral properties of dyes (*E*)-**1**, (*E*)-**2** and their mixtures with excess CB[7] in water.

Compound	λ_{max}^{abs} (nm)	$\lambda_{max}^{fl.ex}$ (nm)	λ_{max}^{fl} (nm)	φ^{fl}
(*E*)-**1**	445	475	600	0.005
(*E*)-**2**	455	490	590	0.01
(*E*)-**1**/CB[7][a]	475	485	595	0.04
(*E*)-**2**/CB[7][a]	485	490	585	0.3

[a] $C_{CB[7]}/C_{dye}$ is 10 for absorption spectra and 50 for fluorescent spectra.

with blue shift of a maximum which reached 7 and 16 nm for dyes **1** and **2**, respectively.

The HypSpec program was used to analyze dependencies of measured absorption and fluorescence spectra upon the changes in concentration of CB[7] with the following evaluation of the spectra and stability constants of complexes dye@CB[7]. The standard deviation, σ_D or σ_I, was used as the criteria of the validity. The results are compiled in Table 2.

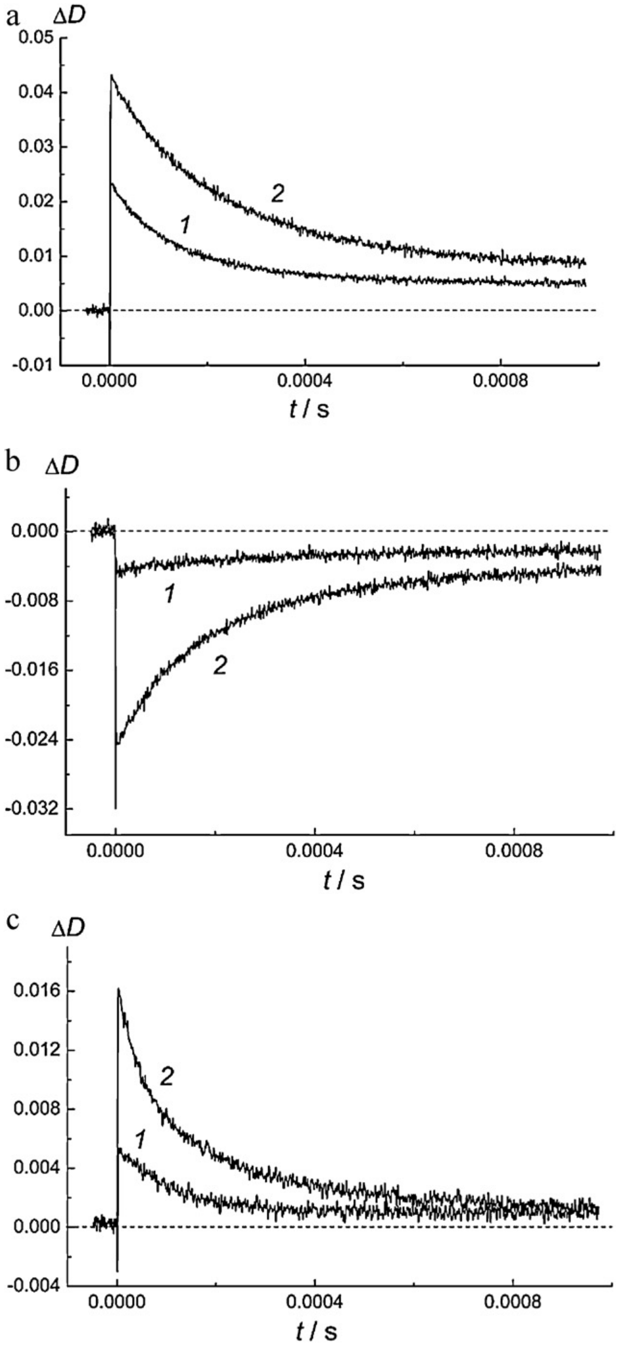

Fig. 11. Kinetics of transient absorption of dye **2** ($C_2 = 2 \times 10^{-5}$ mol L^{-1}) in oxygen-free aqueous solution (1) in the absence and (2) presence of CB[7] ($C_{CB[7]} = 2 \times 10^{-4}$ mol L^{-1}) upon laser pulse at (a) 430, (b) 530 and (c) 670 nm.

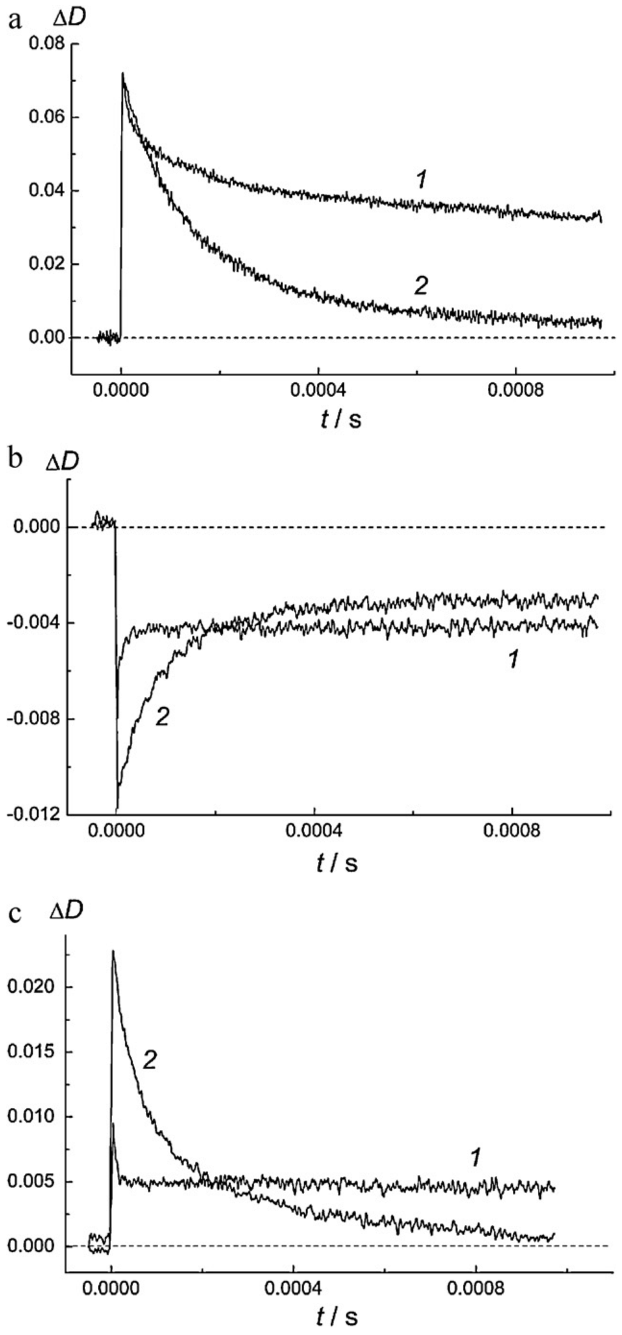

Fig. 12. Kinetics of transient absorption of dye **1** ($C_1 = 2 \times 10^{-5}$ mol L^{-1}) (1) in air-saturated and (2) oxygen-free aqueous solution in the presence of CB[7] ($C_{CB[7]} = 2 \times 10^{-4}$ mol L^{-1}) at (a) 440, (b) 500, and (c) 670 nm.

In all cases the value σ_D is lower than 0.001 (in absorbance units) and σ_I is lower than 0.5% of observed maximal fluorescence intensity (I_{max}), which indicates that the 1:1 complexation model assumed for dyes (*E*)-**1** and (*E*)-**2** is valid. The values of stability constants measured with both methods are similar for dyes **1** and **2** (log$K$ = 3.94–4.11). A moderate decrease in stability constant values with respect to that found from ^{1}H NMR titration (log$K$ = 4.3 and 4.4) is probably due to different conditions of the titration experiments. The main differences are the use of a buffer (0.01 M Li_2CO_3)

Table 2
Spectral properties of dyes (*E*)-**1**, (*E*)-**2**, complexes (*E*)-**1**@CB[7], (*E*)-**2**@CB[7] and stability constants.[a]

Spectrophotometric titration							
Compound	Dye		Dye@CB[7]				
	λ_{max} (nm)	ε_{max} (L mol^{-1} cm^{-1})	λ_{max} (nm)	ε_{max}, (L mol^{-1} cm^{-1})	$\Delta\lambda_{max}$ (nm)[b]	Log*K*[c]	σ_D[d]
(*E*)-**1**	455	27100	476	23400	21	4.02	0.0003
(*E*)-**2**	459	35700	484	34500	25	3.94	0.0003
Fluorescent titration[e]							
Compound	Dye			Dye@CB[7]			
	λ^{fl}_{max} (nm)	I_{max}, a.u.	λ^{fl}_{max} (nm)	I_{max}, a.u.	*Q*[f]	Log*K*[c]	σ_I[d]
(*E*)-**1**	604	5.64	597	156.06	25.0	3.94	0.43
(*E*)-**2**	601	26.71	585	676.74	23.4	4.11	1.51

[a] 0.01 M Li_2CO_3 in the mixture of water–MeCN (10:1, v/v) at room temperature.
[b] $\Delta\lambda_{max} = \lambda_{max}$ (complex) − λ_{max}(free dye).
[c] K = [dye@CB[7]]/{[dye]·[CB[7]]} (L mol^{-1}); the error of the stability constant determination is ±20%.
[d] Standard deviation (in absorbance units for σ_D and in arbitrary units for σ_I) for modeling the absorption and fluorescence spectra, respectively.
[e] Excitation of fluorescence is at 480 nm.
[f] The ratio of values of integrated fluorescence intensity of dye@CB[7] and free dye in the range of 500–700 nm.

and lower concentration of reactants (10^{-5} to 10^{-4} mol L^{-1}), as well as the use of common solvents instead of deuterated ones.

3.5. *Laser pulse photolysis*

The laser excitation of solutions of dyes **1** and **2** and their complexes with CB[7] induces short-term reversible changes in the absorption spectra, which are shown in Fig. 9. It follows from these data that the difference spectra measured in the absence and in the presence of CB[7] are similar. The differences are in the magnitude of the optical density change (ΔD) and in the slight shift in the absorption maxima. In the difference absorption spectra, three characteristic wavelengths can be distinguished: 440, 500 and 670 nm.

The absorption at 430–440 nm may be attributed to *E*–*Z* photoisomerization, the dye triplet and protonation of the dye. The addition of CB[7] to an aqueous solution is known to decrease the pH [48]. Measurement of the acidity of a solution of (*E*)-**1**/CB[7] mixture at $C_{CB[7]} = 2 \times 10^{-4}$ mol L^{-1} showed the pH = 4.2, whereas for a solution of (*E*)-**1** this value is 6.1. The wide band at 600–800 nm is caused by the triplet–triplet (T–T) absorption of the dye. The effect of pH on the difference absorption spectrum of the dye measured upon laser excitation was studied. Fig. 10 shows the difference absorption spectra of **1** in the presence of perchloric acid. A decrease in the pH value entails an increase in ΔD at 400–450 nm and a decrease in ΔD at 600–700 nm. That is, the formation of the protonated form of the dye reduces the probability of intersystem crossing.

Fig. 11 shows the kinetic curves for the oxygen-free solution of **2** and **2**@CB[7]. The curves in Fig. 11a and c demonstrate fast growth of ΔD at 430 and 670 nm for triplet **2**@CB[7] molecules as compared with free **2**; Fig. 11b shows a bleaching at 530 nm. The lifetimes, τ_T, of the triplet of dye **1** and complex **1**@CB[7] are 110 and 140 μs, respectively, and are about equal to τ_T for **2** and **2**@CB[7].

From the analysis of kinetic curves it follows an increase in the efficiency of the intersystem crossing of the dye in the presence of CB[7]. The kinetic curves in Fig. 12 demonstrates the effect of oxygen on the photochemical reactions that occur upon laser excitation of the complex (*E*)-**1**@CB[7]. In the presence of oxygen, a relatively long-lived intermediate is formed which can be attributed to the *Z* isomer. Thus, isomerization occurs in the excited singlet state of the dye. In the absence of oxygen, T–T absorption of the dye takes place and, hence, the yield of the *Z* isomer decreases.

The lifetime of the triplet state of dye **2** and **2**@CB[7] was found to be similar for air saturated solutions (2×10^{-7} s) indicating that the efficiency of the quenching of the triplet state by oxygen is not influenced by the presence of CB[7].

4. Conclusions

The formation of host–guest pseudorotaxane complexes of styryl dyes having dimethylamino group or azacrown-ether residue with CB[7] was found to reduce the conformational mobility of the dye molecule and to result in its relative isolation by the cavitand molecule. In turn, this induces an increase in both the dye luminescence and the probability of the intersystem crossing.

Acknowledgements

This work was supported by the Russian Foundation for Basic Research (Project Nos. 12-03-00107 and 12-03-00491) and the Presidium of the Russian Academy of Sciences. The structural files for quantum chemical calculations were prepared using the program modules developed at the Photochemistry Center of the Russian Academy of Sciences within the State Contract No. 02.523.11.3014.

References

[1] S.P. Gromov, M.V. Alfimov, Supramolecular organic photochemistry of crown-ether-containing styryl dyes, Russian Chemical Bulletin 46 (1997) 611–636.
[2] O.A. Fedorova, YuV. Fedorov, E.N. Andryukhina, S.P. Gromov, M.V. Alfimov, R. Lapouyade, Photochemical electrocyclization of the indolinylphenylethenes involving a C—N bond formation, Organic Letters 5 (2003) 4533–4535.
[3] M.V. Alfimov, S.P. Gromov, O.B. Stanislavskii, E.N. Ushakov, O.A. Fedorova, Crown-containing styryl dyes. 8. Cation-dependent concerted [2 + 2]-autophotocycloaddition of photochromic 15-crown-5 ether betaines, Russian Chemical Bulletin 42 (1993) 1385–1389.
[4] A.I. Vedernikov, L.G. Kuz'mina, S.K. Sazonov, N.A. Lobova, P.S. Loginov, A.V. Churakov, YuA. Strelenko, J.A.K. Howard, M.V. Alfimov, S.P. Gromov, Styryl dyes. Synthesis and study of the solid state [2 + 2] autophotocycloaddition by NMR spectroscopy and X-ray diffraction, Russian Chemical Bulletin International Edition 56 (2007) 1860–1883.
[5] S.P. Gromov, Molecular meccano for light-sensitive and light-emitting nanosized systems based on unsaturated and macrocyclic compounds, Russian Chemical Bulletin International Edition 57 (2008) 1325–1350.
[6] H. Görner, H. Gruen, Photophysical properties of quaternary salts of 4-dialkylamino-4′-azastilbenes and their quinolinium analogues in solution: IX, Journal of Photochemistry 28 (1985) 329–350.
[7] A.V. Barzykin, M.A. Fox, E.N. Ushakov, O.B. Stanislavsky, S.P. Gromov, O.A. Fedorova, M.V. Alfimov, Dependence of metal ion complexation and intermolecular aggregation on photoinduced geometric isomerism in a crown ether styryl dye, Journal of the American Chemical Society 114 (1992) 6381–6385.
[8] E.N. Ushakov, S.P. Gromov, O.A. Fedorova, M.V. Alfimov, Crown-containing styryl dyes. 19. Complexation and cation-induced aggregation of chromogenic aza-15-crown-5 ethers, Russian Chemical Bulletin 46 (1997) 463–471.
[9] S.P. Gromov, E.N. Ushakov, O.A. Fedorova, V.A. Soldatenkova, M.V. Alfimov, Crown ether styryl dyes. 22. Synthesis and complexation of the *cis*-isomers of photochromic aza-15-crown-5 ethers, Russian Chemical Bulletin 46 (1997) 1143–1148.

[10] L.S. Atabekyan, A.K. Chibisov, M.V. Alfimov, Pulse photolysis of crown ether styryl dyes and their complexes with metal ions, High Energy Chemistry 31 (1997) 344–348.

[11] O.A. Fedorova, E.Yu. Chernikova, YuV. Fedorov, E.N. Gulakova, A.S. Peregudov, K.A. Lyssenko, G. Jonusauskas, L. Isaacs, Cucurbit[7]uril complexes of crown-ether derived styryl and (bis)styryl dyes, Journal of Physical Chemistry B 113 (2009) 10149–10158.

[12] A.C. Bhasikuttan, H. Pal, J. Mohanty, Cucurbit[*n*]uril based supramolecular assemblies: tunable physico-chemical properties and their prospects, Chemical Communications 47 (2011) 9959–9971.

[13] R.N. Dsouza, U. Pischel, W.M. Nau, Fluorescent dyes and their supramolecular host/guest complexes with macrocycles in aqueous solution, Chemical Reviews 111 (2011) 7941–7980.

[14] G. Parvari, O. Reany, E. Keinan, Applicable properties of cucurbiturils, Israel Journal of Chemistry 51 (2011) 646–663.

[15] S.P. Gromov, A.I. Vedernikov, L.G. Kuz'mina, D.V. Kondratuk, S.K. Sazonov, Yu.A. Strelenko, M.V. Alfimov, J.A.K. Howard, Photocontrolled molecular assembler based on cucurbit[8] uril: [2 + 2]-autophotocycloaddition of styryl dyes in the solid state and in water, European Journal of Organic Chemistry (2010) 2587–2599.

[16] D.A. Ivanov, N.Kh. Petrov, E.A. Nikitina, M.V. Basilevsky, A.I. Vedernikov, S.P. Gromov, M.V. Alfimov, The 1 host–guest complexation between cucurbit[7]uril and styryl dye, Journal of Physical Chemistry A 115 (2011) 4505–4510.

[17] Z. Li, S. Sun, F. Liu, Y. Pang, J. Fan, F. Song, X. Peng, Large fluorescence enhancement of a hemicyanine by supramolecular interaction with cucurbit[6] uril and its application as resettable logic gates, Dyes and Pigments 93 (2012) 1401–1407.

[18] S.S. Jaffer, P. Ghosh, P. Purkayastha, Mechanistic pathway for controlled extraction of guest molecule bound to herring sperm DNA using α-cyclodextrin, Spectrochimica Acta Part A 78 (2011) 1587–1591.

[19] C. Qin, W. Zhang, Z. Wang, M. Zhou, X. Wang, G. Chen, Optical properties of stilbene-type dyes containing various terminal donor and acceptor groups, Optics Materials 30 (2008) 1607–1615.

[20] M. Sowmiya, P. Purkayastha, A.K. Tiwari, S.S. Jaffer, S.K. Saha, Characterization of guest molecule concentration dependent nanotubes of β-cyclodextrin and their secondary assembly: study with *trans*-2-[4-(dimethylamino)styryl]benzothiazole, a TICT-fluorescence probe, Journal of Photochemistry and Photobiology A: Chemistry 205 (2009) 186–196.

[21] I. Suzuki, C. Nakayama, M. Ui, K. Hirose, A. Yamauchi, Greater fluorescence from styrylpyridinium dye upon complexation with cyclodextrin derivatives through a *p*–*p* interaction, Analytical Sciences 23 (2007) 249–251.

[22] J.W. Park, K.H. Park, Inclusion of (aminostyryl)-l-methylpyridinium dyes by β-cyclodextrin and its use for fluorescent-probe studies on association of cationic and neutral molecules with β-cyclodextrin, Journal of Inclusion Phenomena Molecular Recognition Chemistry 17 (1994) 277–290.

[23] Yu.V. Fedorov, O.A. Fedorova, E.N. Andryukhina, S.P. Gromov, M.V. Alfimov, J.J. Aaron, Guest–host interactions between crown-containing 2-styrylbenzothiazole and HP-β-CD, Journal of Inclusion Phenomena Macrocyclic Chemistry 49 (2004) 283–289.

[24] P. Purkayastha, Cu^{2+} induced charge transfer switch by choosing the right cyclodextrin environment, Journal of Photochemistry and Photobiology A: Chemistry 212 (2010) 43–48.

[25] U. Narang, C.F. Zhao, J.D. Bhawalkar, F.V. Bright, P.N. Prasad, Characterization of a new solvent-sensitive two-photon-induced fluorescent (aminostyryl)pyridinium salt dye, Journal of Physical Chemistry 100 (1996) 4521–4525.

[26] P. Purkayastha, D. Das, S.S. Jaffer, Differential encapsulation of *trans*-2-[4-(dimethylamino)styryl]benzothiazole in cyclodextrin hosts: application towards nanotubular suprastructure formation, Journal of Molecular Structure 892 (2008) 461–465.

[27] D. Sahoo, S. Chakravorti, Orientational dynamics of a charge transfer complex in cyclodextrin cavity as receptor, Physical Chemistry Chemical Physics 10 (2008) 5890–5897.

[28] L.S. Atabekyan, N.A. Lobova, A.I. Vedernikov, S.P. Gromov, A.K. Chibisov, Photonics of azacrown-containing styryl dye and its complexes with metal ions: 1. Triplet states, High Energy Chemistry 46 (2012) 100–105.

[29] C. Frassineti, S. Ghelli, P. Gans, A. Sabatini, M.S. Moruzzi, A. Vacca, Nuclear magnetic resonance as a tool for determining protonation constants of natural polyprotic bases in solution, Analytical Biochemistry 231 (1995) 374–382.

[30] J.P. Perdew, K. Burke, M. Ernzerhof, Generalized gradient approximation made simple, Physical Review Letters 77 (1996) 3865–3868.

[31] D.N. Laikov, Fast evaluation of density functional exchange-correlation terms using the expansion of the electron density in auxiliary basis sets, Journal of Chemical Physics 281 (1997) 151–156.

[32] D.N. Laikov, YuA. Ustynyuk, PRIRODA-04: a quantum-chemical program suite. New possibilities in the study of molecular systems with the application of parallel computing, Russ. Chem. Bull. Int. Ed. 54 (2005) 820–826.

[33] L.V. Levshin, A.M. Saletsky, Luminescence and Its Measurements, Publishing House of Moscow State University, Moscow, 1989 [in Russian].

[34] P. Gans, A. Sabatini, A. Vacca, Investigation of equilibria in solution. Determination of equilibrium constants with the HYPERQUAD suite of programs, Talanta 43 (1996) 1739–1753.

[35] J.J.P. Stewart, Optimization of parameters for semiempirical methods. 1. Method, Journal of Computational Chemistry 10 (1989) 209–220.

[36] Y. Amatatsu, Skeletal relaxation effect on the charge transfer state formation of 4-dimethylamino, 4′-cyanostilbene, Journal of Physical Chemistry A 110 (2006) 8736–8743.

[37] J.-F. Letard, R. Lapouyade, W. Retting, Structure–photophysics correlations in a series of 4-(dialkylamino)stilbenes: intramolecular charge-transfer in the excited-state as related to the twist around the single bonds, Journal of the American Chemical Society 115 (1993) 2441–2447.

[38] J.-S. Yang, C.-K. Lin, A.M. Lahoti, C.-K. Tseng, Y.-H. Liu, G.-H. Lee, S.-M. Peng, Effect of ground-state twisting on the *trans-cis* photoisomerization and TICT state formation of aminostilbenes, Journal of Physical Chemistry A 113 (2009) 4868–4877.

[39] B.M. Uzhinov, V.L. Ivanov, M.Ya. Mel'nikov, Molecular rotors as luminescence sensors of local viscosity and viscous flow in solutions and organized systems, Russian Chemical Reviews 80 (2011) 1179–1190.

[40] J.-S. Yang, K.-L. Liau, C.-M. Wang, C.-Y. Hwang, Substituent-dependent photoinduced intramolecular charge transfer in *N*-aryl-substituted *trans*-4-aminostilbenes, Journal of the American Chemical Society 126 (2004) 12325–12335.

[41] J.-S. Yang, K.-L. Liau, C.-Y. Li, M.-Y. Chen, Meta conjugation effect on the torsional motion of aminostilbenes in the photoinduced intramolecular charge-transfer state, Journal of the American Chemical Society 129 (2007) 13183–13192.

[42] B.D. Wagner, N. Stojanovic, A.I. Day, R.J. Blanch, Host properties of cucurbit[7]uril: fluorescence enhancement of anilinonaphthalene sulfonates, Journal of Physical Chemistry B 107 (2003) 10741–10746.

[43] W.M. Nau, J. Mohanty, Taming fluorescent dyes with cucurbituril, International Journal of Photoenergy 7 (2005) 133–141.

[44] A.L. Koner, W.M. Nau, Cucurbituril encapsulation of fluorescent dyes, Supramolecular Chemistry 19 (2007) 55–66.

[45] Y.Y. Zhou, H.P. Yu, L. Zhang, J.Y. Sun, L. Wu, Q. Lu, L. Wang, Host properties of cucurbit[7]uril: fluorescence enhancement of acridine orange, Journal of Inclusion Phenomena Macrocyclic Chemistry 61 (2008) 259–264.

[46] M. Megyesi, L. Biczok, I. Jablonkai, Highly sensitive fluorescence response to inclusion complex formation of berberine alkaloid with cucurbit[7]uril, Journal of Physical Chemistry C 112 (2008) 3410–3416.

[47] N.Kh. Petrov, D.A. Ivanov, D.V. Golubkov, S.P. Gromov, M.V. Alfimov, The effect of cucurbit[7]uril on photophysical properties of aqueous solution of 3,3′-diethylthiacarbocyanine iodide dye, Chemical Physics Letters 480 (2009) 96–99.

[48] A.M.M. Rawashdeh, A. Thangavel, C. Sotiriou-Leventis, N. Leventis, Control of the ketone to *gem*-diol equilibrium by host–guest interaction, Organic Letters 10 (2008) 1131–1134.